

# Metal Ion Catalysis by Blocking Inhibitory Reverse Paths in the Hydrolysis of 3-Carboxy aspirin

Junghun Suh\* and Keun Ho Chun

Contribution from the Department of Chemistry, Seoul National University, Seoul 151, Korea.  
Received September 17, 1985

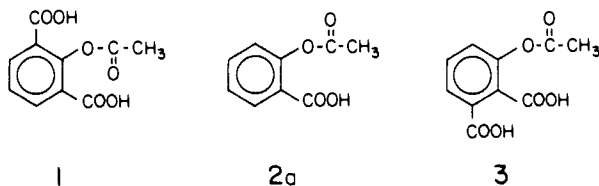
**Abstract:** The hydrolysis of 3-carboxy aspirin (**1**) was kinetically investigated in the presence or absence of tri- or divalent metal ions. The spontaneous hydrolysis of the neutral and the monoanionic forms of **1** involves anhydride intermediates formed by the nucleophilic attack of the carboxyl group at the ester linkage, while that of the dianionic form of **1** proceeds through the general-base catalysis by the carboxylate ion in the attack of a water molecule at the ester group. The reaction rates were markedly increased upon addition of Fe(III) or Al(III) ion. The metal ion catalyzed hydrolysis of the dianionic form as well as the monoanionic form of **1** involves the nucleophilic attack by the carboxyl group, and the resultant anhydride intermediates are complexed by the trivalent metal ions. The complexation of the intermediates leads to the blocking of the inhibitory reverse attack by the phenolate ion of the intermediates at the anhydride group and, consequently, to the enhancement in the overall reaction rates. Rate enhancement by blocking the inhibitory reverse path was especially efficient in the nucleophilic path involving the dianionic form of **1**. Implications of the novel catalytic role of metal ions, catalysis by blocking the inhibitory reverse paths, to the mechanisms of the action of metalloenzymes are also discussed.

Many studies have been performed on metal ion catalysis in organic reactions in which the metal ion acts as a Lewis acid.<sup>1-3</sup> Elucidation of the exact catalytic roles of the metal ions in such reactions is an important subject in the study of both inorganic and organic reaction mechanisms. In addition, catalytic features of metal ions revealed by the studies with small molecules are utilized in assignment of the catalytic roles of metal ions in the action of metalloenzymes.

The catalytic roles of metal ions as Lewis acids, which have been disclosed by previous mechanistic studies, can be grouped into four categories:<sup>1</sup> (I) Attachment of the metal ion on a suitable site on an electrophile enhances the reactivity of the electrophile. (II) Attachment of the metal ion to a departing nucleophile increases its leaving ability. (III) The metal acts as a center for the simultaneous attachment of both an electrophile and the attacking nucleophile, thus converting inter- into an intramolecular process (template effects). (IV) Induced ionization of protons from ambient nucleophiles by metal ions produces improved nucleophiles. In addition, metal ion induced conformational changes can also lead to catalysis in enzymatic systems, although this factor has not been demonstrated with small molecules.

In our previous studies,<sup>4-8</sup> new catalytic features of metal ions have been disclosed. For example, the nucleophilic attack of a metal-bound water molecule at a complexed ester linkage was observed.<sup>4-6</sup> This has been further related to the mechanism of carboxypeptidase A, a metalloprotease.<sup>6,9</sup> Studies with the Zn-(II)-catalyzed hydrolysis of 6-carboxy-2-pyridinecarboxaldehyde acetate revealed that the catalytic unit was binuclear Zn(II) ions.<sup>8</sup>

In this paper, we report the kinetic data for the spontaneous and the metal ion catalyzed hydrolysis of 3-carboxy aspirin (**1**).



Analysis of the kinetic data reveals a novel catalytic factor, metal

ion catalysis by blocking inhibitory reverse paths, that does not belong to the four categories previously listed. Implications of the new catalytic factor to the catalytic roles of metal ions in metalloenzymes are also discussed in this report.

## Experimental Section

**Materials.** 3-Carboxy aspirin (**1**) was prepared by refluxing 3-carboxysalicylic acid<sup>10</sup> (1 g) in acetic anhydride (20 mL) for 3 h. After the mixture was cooled to room temperature, 100 g of ice water was added to the mixture. Several hours later, precipitates were collected and recrystallized from ether-hexane; mp 160-161 °C (lit.<sup>11</sup> 162-163 °C). Dimethyl 3-carboxysalicylate was obtained by refluxing **1** (1 g) in 20 mL of methanol in the presence of 0.1 g of sulfuric acid for 24 h and was purified by recrystallization from ethyl acetate-hexane; mp 68-70 °C. Methyl 3-carboxysalicylate was prepared by the partial hydrolysis of the dimethyl ester in boiling aqueous methanol with added sodium hydroxide. The process of the partial hydrolysis was followed by TLC, and the prepared monomethyl ester was purified by eluting with chloroform on a silica gel column. The product was further purified by recrystallization from acetone-petroleum ether; mp 132-134 °C.

The solutions of the chloride salts of Fe(III), Cu(II), and Zn(II) ion were prepared by dissolving the corresponding oxides (Aldrich, "Gold" Label) with hydrochloric acid. Aluminum chloride was purified by sublimation. Water was redistilled and deionized prior to the preparation of buffer solutions.

**Kinetic Measurements.** Reaction rates were measured with a Beckman 5260 or a Beckman 25 UV/vis spectrophotometer by following absorbance changes at 310 nm [in the spontaneous reaction or in the presence of Cu(II) or Zn(II) ion], 320 nm [in the presence of Al(III) ion], or 470 nm [in the presence of Fe(III) ion]. Temperature was controlled to within 0.1 °C with a Haake E52 or a Lauda Brinkman T-2 circulator. The reactions were carried out in the presence of 0.8% (v/v) acetone at ionic strength 0.6 [0.1 for Fe(III)-containing solutions], which was adjusted with sodium chloride. Buffers (0.01 M) used were chloroacetate (pH 1.7-3.3), formate (pH 3.3-4.2), 2-morpholinoethanesulfonic acid (pH 5.5-7.0), or *N*-(2-hydroxyethyl)piperazine-*N'*-2-ethanesulfonic acid (pH 7.0-8.0). pH measurements were performed with a Fisher Accumet Model 525 pH meter. The concentration of **1** employed in kinetic studies was  $1 \times 10^{-4}$  M unless noted otherwise. Pseudo-first-order rate constants ( $k_0$ ) were calculated with the measured infinity absorbance values. For the reactions with half-lives greater than 1 h, however,  $k_0$  was calculated by the Guggenheim method or by the initial rate method. The quantitative formation of 3-carboxysalicylic acid from the spontaneous or metal ion catalyzed hydrolysis of **1** was evidenced by the UV/vis spectra of the product solutions. Characteristic spectra of the product are obtained especially in the presence of added Fe(III) ion.

## Results

**Spontaneous Hydrolysis of 1.** Rates for the spontaneous hydrolysis of **1** were measured over pH range 0-8 at 60 °C. Kinetic

(1) Satchell, D. P. N.; Satchell, R. S. *Annu. Rep. Prog. Chem., Sect. A: Inorg. Chem.* **1979**, *75*, 25 and references therein.

(2) Dunn, M. F. *Struct. Bonding (Berlin)* **1975**, *23*, 61.

(3) Hipp, C. J.; Busch, D. H. *Coordination Chemistry*; Martell, A. E., Ed.; ACS Monograph 174; American Chemical Society: Washington, DC, 1978; Vol. 2, Chapter 2.

(4) Suh, J.; Lee, E.; Jang, E. S. *Inorg. Chem.* **1981**, *20*, 1932.

(5) Suh, J.; Cheong, M.; Suh, M. P. *J. Am. Chem. Soc.* **1982**, *104*, 1654.

(6) Suh, J.; Han, H. *Bioorg. Chem.* **1984**, *12*, 177.

(7) Suh, J.; Suh, M. P.; Lee, J. D. *Inorg. Chem.* **1985**, *24*, 3088.

(8) Suh, J.; Han, O.; Chang, B. *J. Am. Chem. Soc.* in press.

(9) Suh, J.; Cho, W.; Chung, S. *J. Am. Chem. Soc.* **1985**, *107*, 4530.

(10) Todd, D.; Martell, A. E. *Organic Synthesis*; Baumgarten, H. E., Ed.; Wiley: New York, 1973; Collect. Vol. V, p 617.

(11) Pande, C. S.; Tewari, J. D. *Chem. Ber.* **1962**, *95*, 2623.

**Table I.** Pseudo-First-Order Rate Constants Measured for the Spontaneous Hydrolysis of **1** at pH 0–8

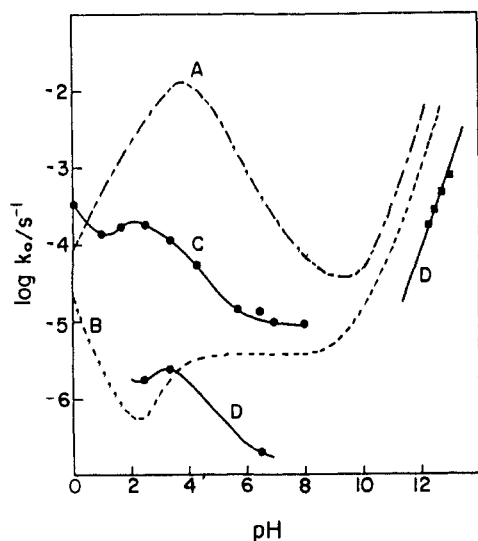
pH <sup>a</sup>	$k_0, 10^{-6} \text{ s}^{-1}$				
	65 °C	60 °C	55 °C	50 °C	25 °C <sup>b</sup>
0.00 <sup>c</sup>		318			
1.00 <sup>c</sup>		145			
1.70		158			
2.50 <sup>d</sup>	261	162	87.7	45.3	1.67
3.30 <sup>d</sup>	180	116	70.0	41.3	2.56
4.20		54.5			
5.70		14.9			
6.50 <sup>d</sup>	24.0	14.1	7.61	4.70	0.201
7.00		9.66			
8.00		9.96			

<sup>a</sup> pH values measured at 25 °C. <sup>b</sup> Calculated from the temperature dependence of  $k_0$  measured at higher temperatures. <sup>c</sup> Taken as  $-\log [\text{H}^+]$ . <sup>d</sup> The values of  $E_a$  (kcal/mol),  $\Delta H^\ddagger$  (kcal/mol),  $\Delta G^\ddagger$  (kcal/mol), and  $\Delta S^\ddagger$  (cal/mol-deg) at 25 °C are  $25.5 \pm 1.0$ ,  $24.9 \pm 1.0$ ,  $25.3$ , and  $-1.2 \pm 3.5$ , respectively, for the data at pH 2.50,  $21.4 \pm 0.4$ ,  $20.8 \pm 0.4$ ,  $25.0$ , and  $-14.1 \pm 1.4$ , respectively, for the data at pH 3.30, and  $23.9 \pm 0.9$ ,  $23.3 \pm 0.9$ ,  $26.5$ , and  $-10.7 \pm 2.9$ , respectively, for the data at pH 6.50. Since more than two reaction paths are involved at each of these pHs, the values of the activation parameters are not mechanistically meaningful.

**Table II.** Second-Order Rate Constants for the Alkaline Hydrolysis of Various Aspirin Derivatives

compd	$k_{\text{OH}}, \text{M}^{-1} \text{ s}^{-1}$	temp, °C
3-carboxyaspirin ( <b>1</b> )	$9.12 \times 10^{-3}$	25
aspirin ( <b>2a</b> ) <sup>a</sup>	0.11	25
3,5-dinitroaspirin <sup>b</sup>	15.3	39
6-carboxyaspirin ( <b>3</b> ) <sup>c</sup>	0.42	25

<sup>a</sup> Reference 12. <sup>b</sup> Reference 13. <sup>c</sup> Reference 14.

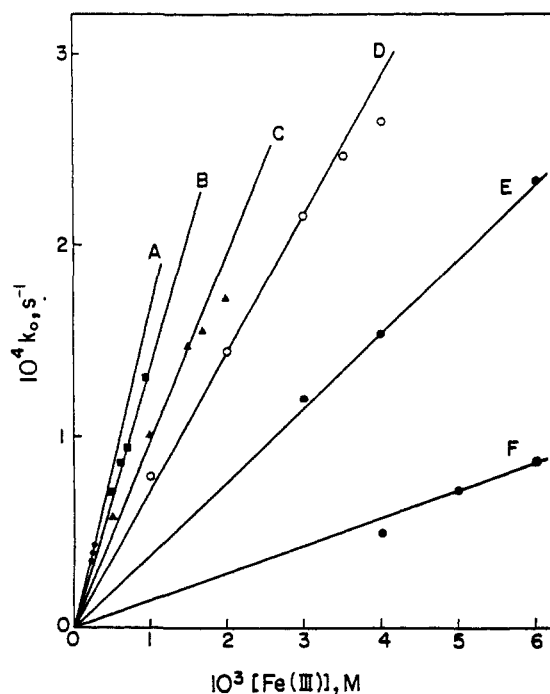
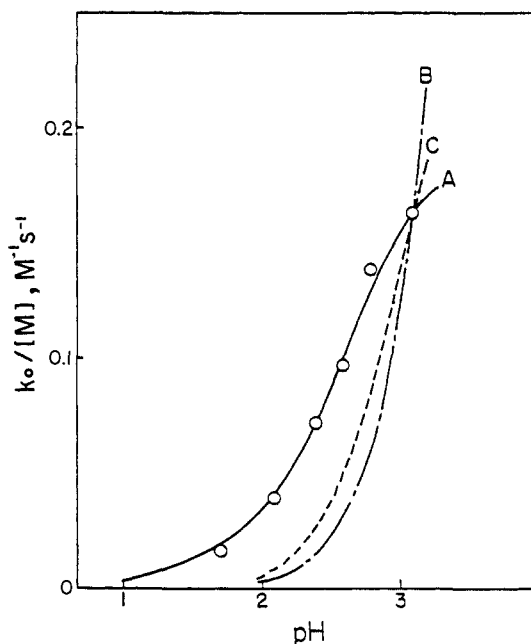
**Figure 1.** Plot of  $\log k_0$  against pH for the spontaneous hydrolysis of **1** at 60 °C (curve C) or 25 °C (curve D), **2a** at 25 °C (curve B),<sup>12</sup> or **3** at 25 °C (curve A).<sup>14</sup>

data at pH 2.5, 3.3, and 6.5 were also obtained at various temperatures. The pseudo-first-order rate constants ( $k_0$ ) thus obtained are summarized in Table I. The  $k_0$  values at 25 °C were estimated from the Arrhenius plots of the rate data measured at higher temperatures and are also listed in this table. Rates for the alkaline hydrolysis of **1** were measured with 0.02–0.1 N sodium hydroxide. In Table II, the values of the second-order rate constants for the alkaline hydrolysis of various aspirin derivatives are compared. The rate data obtained for the spontaneous hydrolysis of **1** are illustrated in Figure 1. The rate data previously reported for the hydrolysis of aspirin (**2a**)<sup>12</sup> and 6-carboxyaspirin (**3**)<sup>14</sup> are also illustrated in this figure.

(12) Garrett, E. R. *J. Am. Chem. Soc.* **1957**, *79*, 3401.

(13) Fersht, A. R.; Kirby, A. J. *J. Am. Chem. Soc.* **1968**, *90*, 5818.

(14) Fersht, A. R.; Kirby, A. J. *J. Am. Chem. Soc.* **1968**, *90*, 5833.

**Figure 2.** Plot of  $k_0$  against  $[\text{Fe(III)}]$  for the Fe(III)-catalyzed hydrolysis of **1** at various pHs and 25 °C: A, pH 3.10; B, pH 2.80; C, pH 2.60; D, pH 2.40; E, pH 2.10; F, pH 1.70.**Figure 3.** pH profile of the slope ( $k_0/[\text{M}]$ ) of the straight lines illustrated in Figure 2. Curve A is constructed according to eq 4 by using  $k_{11}k_{11}^{-1}/k_{-11}^{-1} = 0.29 \text{ M}^{-1} \text{ s}^{-1}$  and the  $\text{p}K_{11}$  (2.85) and  $\text{p}K_{12}$  (3.80) values reported in ref 19. Curve B represents a typical curve based on eq 5. Curve C is based on an equation analogous to eq 4 except that the  $k_{-1}[\text{H}^+]$  term is assumed to be equal to  $k_{12}^{\text{M}}$  at pH 3. The reported<sup>19</sup> values of  $\text{p}K_{11}$  and  $\text{p}K_{12}$  are used in the construction of curves B and C.

**Metal Ion Catalyzed Hydrolysis of **1**.** The Fe(III)-catalyzed hydrolysis of **1** was kinetically examined at pH 1.7–3.1. The  $k_0$  values obtained at various pHs are plotted against  $[\text{Fe(III)}]$  in Figure 2. Because of the limited solubility of Fe(III) ion in the buffer solutions, the kinetic measurements were performed over the  $[\text{Fe(III)}]$  and pH ranges indicated in this figure. The slopes of the straight lines drawn in Figure 2 are plotted against pH in Figure 3.

The Al(III)-catalyzed hydrolysis of **1** was studied at pH 2.1–4.2 at 25 °C, and the results are illustrated in Figure 4. Again the solubility of the metal ion did not allow kinetic measurements at

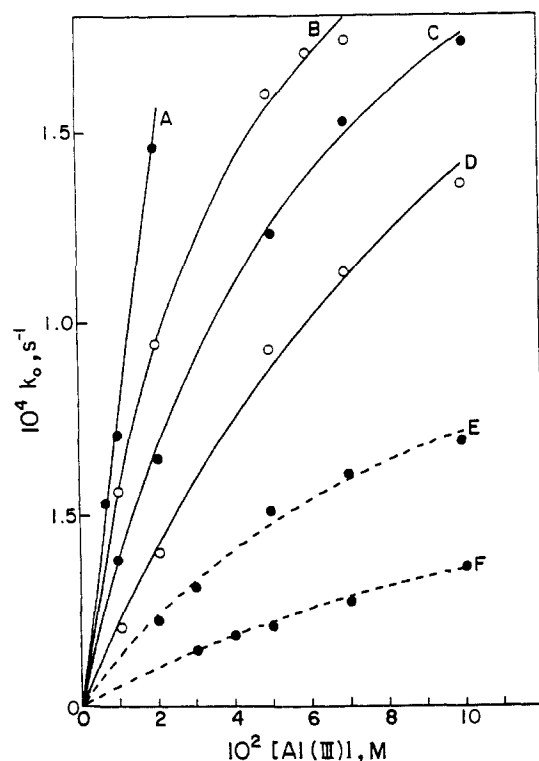


Figure 4. Plot of  $k_0$  against  $[Al(III)]$  for the  $Al(III)$ -catalyzed hydrolysis of **1**: A, pH 4.20; B, pH 3.80; C, pH 3.30; D, pH 2.90; E, pH 2.50; F, pH 2.10.

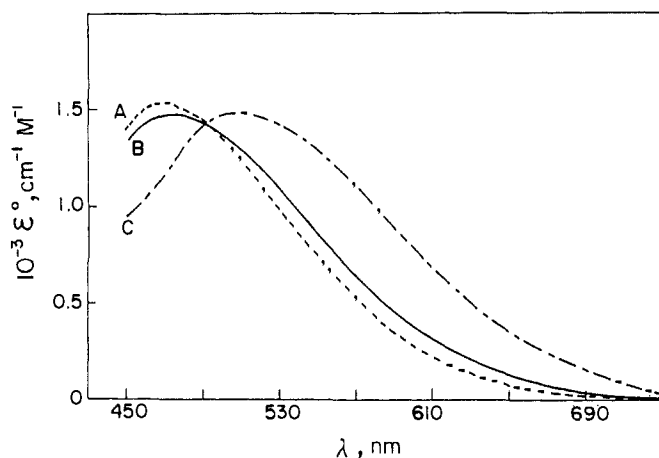


Figure 5. Product spectrum (curve B) for the solvolysis of **1** ( $3 \times 10^{-4}$  M) in the presence of 0.003 M  $Fe(III)$  ion at pH 2.40 and 25 °C in 50% (v/v) aqueous methanol. Curve A represents the spectrum of 3-carboxysalicylic acid and curve C that of methyl 3-carboxysalicylate under identical conditions.

higher  $[Al(III)]$  or pHs than those indicated in Figure 4.

The hydrolysis of **1** was also examined in the presence of 0.01 M  $Cu(II)$  or 0.01 M  $Zn(II)$  ion at pH 3.3 and 50 °C. The  $k_0$  values observed were  $6.3 \times 10^{-5}$ ,  $4.6 \times 10^{-5}$ , and  $4.1 \times 10^{-5} s^{-1}$ , respectively, for the reaction in the presence of  $Cu(II)$  ion, for that in the presence of  $Zn(II)$  ion, and for the spontaneous reaction. Therefore, the catalysis by the bivalent ions is negligible in contrast with that by the trivalent metal ions.

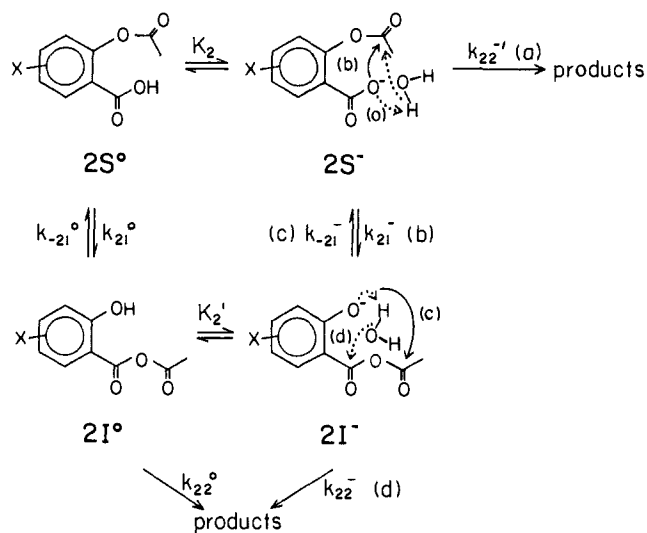
Changes in buffer concentrations (0.01–0.1 M chloroacetate for the spontaneous reaction at pH 2.50 and 60 °C, 0.005–0.02 M chloroacetate for the  $Fe(III)$ -catalyzed reaction at pH 2.80 and 25 °C, and 0.01–0.05 M formate for the  $Al(III)$ -catalyzed reaction at pH 3.80 and 25 °C) did not affect  $k_0$  values for the spontaneous or metal ion catalyzed hydrolysis of **1** appreciably. The hydrolysis of the unsubstituted aspirin (**2a**) was examined in the presence of  $Fe(III)$  ion (0.015 M at pH 2.1, 0.001 M at pH 2.8), but no appreciable catalysis was detected.

Table III. Solvolysis Products for Aspirin Derivatives Obtained in 1:1 (v/v) Water–Methanol

compd	conditions	amt of mono-methyl ester, %
<b>1</b> <sup>a</sup>	spontaneous, pH 3.3, <sup>b</sup> 60 °C	10.5 ± 0.5
<b>1</b> <sup>c</sup>	spontaneous, pH 8.0, <sup>b</sup> 60 °C	ca. 0
<b>1</b> <sup>d</sup>	0.001 M $Fe(III)$ , pH 2.4, <sup>b</sup> 25 °C	20.0 ± 1.0
3,5-dinitroaspirin <sup>e,f</sup>	acid form, 39 °C	12.2 ± 0.7
3,5-dinitroaspirin <sup>g</sup>	anion form, 39 °C	60 ± 2

<sup>a</sup>  $k_0$  was  $1.76 \times 10^{-4} s^{-1}$  in the presence of 50% (v/v) methanol while it was  $1.16 \times 10^{-4} s^{-1}$  in the absence of methanol at pH 3.3 and 60 °C. <sup>b</sup> pH values were measured in the presence of the added methanol. <sup>c</sup>  $k_0$  at pH 8.0 was  $4.99 \times 10^{-5} s^{-1}$  while that at pH 9.0 was  $4.88 \times 10^{-5} s^{-1}$ , indicating that the reaction at these pHs represents the hydrolysis of the dianionic form of **1**.  $k_0$  at pH 8.0 in the absence of methanol was  $9.96 \times 10^{-6} s^{-1}$ . At pH 8.0 and 60 °C, the monomethyl ester of 3-carboxysalicylate was not hydrolyzed appreciably when examined up to 24 h. <sup>d</sup>  $k_0$  was  $7.78 \times 10^{-5} s^{-1}$  in the presence of 50% (v/v) methanol while that in the absence of methanol was  $1.66 \times 10^{-5} s^{-1}$ . <sup>e</sup> Reference 16. <sup>f</sup> The spectral data used in the quantitation of the methyl ester of 3,5-dinitrosalicylate are reported in ref 16. The spectral properties of the methyl ester and the salicylate employed for **1** in the present study are better suited for the spectroscopic quantitation than those reported in ref 16. <sup>g</sup> Reference 13.

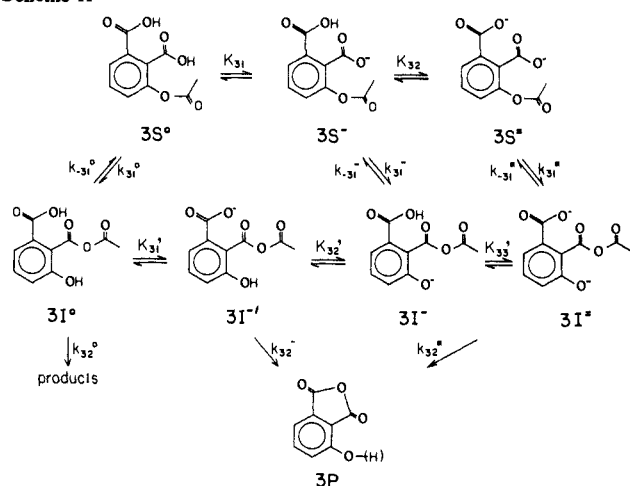
#### Scheme I



**Solvolysis Products.** Solvolysis products were examined in 1:1 (v/v) aqueous methanol for the  $Fe(III)$ -catalyzed or the spontaneous hydrolysis of **1**. The quantitation of the monomethyl ester of 3-carboxysalicylic acid was performed with the visible spectra of the product solutions. Reliable results were obtained by comparing the spectra of the  $Fe(III)$  complexes of 3-carboxysalicylic acid and its monomethyl ester. In Figure 5, the spectrum of the product solution for a  $Fe(III)$ -catalyzed reaction is compared with those of 3-carboxysalicylic acid and the monomethyl ester. From the absorbance values measured at several wavelengths, the amount of the monomethyl ester present in the product solution was calculated. For the spontaneous reaction,  $Fe(III)$  ion was added to the product solutions after completion of the reaction in order to quantitate the monomethyl ester as the  $Fe(III)$  complex.<sup>15</sup> The results for the quantitation of the solvolysis products are summarized in Table III. In this table, the solvolysis products are compared with those of 3,5-dinitroaspirin.

(15) For the  $Al(III)$ -catalyzed reactions, correct quantitation of the monomethyl ester was not achieved even by the addition of  $Fe(III)$  ion after the completion of the reaction. This is apparently because the limited solubility of  $Fe(III)$  ion did not allow the addition of a sufficient amount of  $Fe(III)$  ion that can compete with a large concentration of  $Al(III)$  ion for complex formation with the products.

Scheme II



## Discussion

**Mechanism of the Spontaneous Hydrolysis of 1.** The mechanism (Scheme I) of the hydrolysis of various derivatives of aspirin has been intensively investigated.<sup>12-14,16-18</sup> In general, aspirin anion derivatives ( $2S^-$ ) are hydrolyzed through the intramolecular general-base catalysis ( $k_{22}^-$  path) by the carboxylate ion.<sup>17,18</sup> Although a nucleophilic path involving  $2I^-$  is available for the hydrolysis of  $2S^-$ , the very efficient reverse attack ( $k_{-21}^-$  step;  $2I^- \rightarrow 2S^-$ ) of the phenolate ion at the anhydride group in  $2I^-$  lowers the concentration of  $2I^-$ , reducing the overall rate of the nucleophilic path. However, reduction of the basicity of the phenolate ion as exemplified by the introduction of 3,5-dinitro groups suppresses the reverse attack of the phenolate ion, changing the mechanism to the nucleophilic one.<sup>13</sup> In this case, the breakdown ( $k_{22}^-$  step) of  $2I^-$  is the rate-determining step, which is subject to general-base catalysis by the phenolate group. For aspirin acid derivatives,<sup>16</sup> the phenolate group of  $2I^0$ , an intermediate formed in the nucleophilic mechanism, is protonated, and, thus, its reverse attack at the anhydride group is blocked. On the other hand, the general-base catalysis by the carboxylate group in the attack of water at the ester linkage is not available for  $2S^0$ . Consequently, the un-ionized form of aspirin acid derivatives are hydrolyzed through the nucleophilic mechanism. The rate-determining step for the hydrolysis of the aspirin acid derivatives is the breakdown of  $2I^0$  ( $k_{22}^0$  step).

The hydrolysis rate was remarkably enhanced when the 6-carboxy group was introduced to aspirin (Scheme II).<sup>14</sup> In the reaction of the monoanionic species ( $3S^-$ ), the reverse attack by the phenolate ion at the anhydride group of  $3I^-$  is blocked by the intramolecular proton transfer that produces  $3I^{-'}$ . The intramolecular reaction of  $3I^{-'}$  to produce  $3P$  is very effective, and the overall rate was very fast, with the rate-determining step being the  $k_{31}^-$  step ( $3S^- \rightarrow 3I^-$ ). For the reaction of the dianionic species ( $3S^{2-}$ ), the reverse attack ( $k_{-31}^{2-}$  step;  $3I^{2-} \rightarrow 3S^{2-}$ ) by the phenolate ion at the anhydride group should be very fast, decreasing the concentration of  $3I^{2-}$ . However, the  $k_{32}^{2-}$  step ( $3I^{2-} \rightarrow 3P$ ) involves very efficient intramolecular attack by the carboxyl group, making the hydrolysis of  $3S^{2-}$  to proceed through the nucleophilic mechanism. The neutral species ( $3S^0$ ) is hydrolyzed through the nucleophilic mechanism involving the intermediacy of  $3I^0$ , just as in the hydrolysis of other aspirin acid derivatives.

In summary, aspirin derivatives are hydrolyzed through the nucleophilic mechanism when the inhibitory reverse attack of phenolate ions in the anhydride intermediates is suppressed, or the breakdown of the anhydride intermediates is greatly catalyzed. The mechanism of the spontaneous or metal-catalyzed hydrolysis of **1** can be discussed in terms of the mechanistic information provided by Schemes I and II.

The rate data measured at pH <8 for the spontaneous hydrolysis of **1** reflect ionization of the two carboxyl groups ( $pK_{a1} = 2.85$ ,  $pK_{a2} = 3.80$ ).<sup>19</sup> The reaction paths at pH <8 and 60 °C (Figure 1) can be assigned as the reaction of the neutral form of **1** with the external specific acid (pH <1) and the intramolecular reactions of the neutral (pH ~1), monoanionic (pH ~3), and dianionic (pH 6–8) forms of **1**. The rate of the intramolecular reaction of the dianionic species is much slower than that of the monoanionic one, while those of the neutral and the monoanionic species are comparable to each other.

The dianionic species ( $1S^{2-}$ ) should be hydrolyzed through the general-base mechanism ( $k_{12}^{2-}$  step of Scheme III) since the reverse attack by the phenolate ion ( $k_{-11}^{2-}$  step;  $1I^{2-} \rightarrow 1S^{2-}$ ) is very efficient as in the hydrolysis of unsubstituted aspirin anion.

In the reaction of the monoanionic species ( $1S^-$ ), the reverse attack by the phenolate ion of  $1I^-$  ( $k_{-11}^-$  step;  $1I^- \rightarrow 1S^-$ ) is blocked by the intramolecular proton transfer ( $k_1$  step), which leads to the formation of  $1I^{-'}$ . Therefore,  $1S^-$  would be hydrolyzed through the intermediacy of  $1I^{-'}$ . Since no catalytic path is available for the breakdown of  $1I^{-'}$ , the rate-determining step in the hydrolysis of  $1S^-$  should be the breakdown of  $1I^{-'}$  ( $k_{12}^-$  step), as in the hydrolysis of aspirin acid derivatives. Whether  $1I^{-'}$  is produced directly from  $1S^-$  (i.e., general-acid catalysis by the un-ionized carboxyl group in  $1S^-$ ) or through  $1I^0$  is unclear.

The reaction of the neutral species ( $1S^0$ ) would proceed through the nucleophilic mechanism as those of other aspirin acid derivatives. The similar rates of  $1S^0$  and  $1S^-$  (Figure 1) are compatible with the reaction paths involving  $1I^0$  and  $1I^{-'}$ .<sup>20</sup>

Further support for the mechanism of Scheme III comes from the solvolysis products (Table III) of **1** obtained in the presence of 50% (v/v) methanol. Formation of the monomethyl ester of 3-carboxysalicylic acid in 10% yield at pH 3.30 indicates the trapping<sup>13,16</sup> of the anhydride intermediate by methanol in the reaction of  $1S^-$ . The failure to detect the monomethyl ester in the hydrolysis of **1** at pH 8 supports the general-base mechanism for  $1S^{2-}$ .

The alkaline hydrolysis of **1** (Table II) is much slower than that of **2a** or **3**. The rate of the hydrolysis of  $1S^{2-}$  at pH 6–8 (Figure 1, curve D) is also much slower than that of unsubstituted aspirin anion at pH 6–8 (Figure 1, curve B) although both of these reactions proceed through the general-base mechanism. Examination of the space-filling models indicates that the approach of an external hydroxide ion or a water molecule to the acetoxy group of **1** is protected by the two carboxyl groups when the stable conformations of **1** are considered. This explains the very low rates of the alkaline hydrolysis and the general-base path of  $1S^{2-}$  compared with those of **2a** or **3**. The models, however, indicate that the attack of the carboxylate at the acetoxy group ( $k_{11}^-$ ,  $k_{11}^{-'}$ , or  $k_{11}^{2-}$  step) and the intramolecular proton transfer in  $1I^-$  ( $k_1$  step) are not influenced appreciably by the steric effects of the other carboxyl group.

**Mechanism of the Metal Ion Catalyzed Hydrolysis of 1.** Sites for chelation by metal ions are not available in  $1S^0$ ,  $1S^-$ , or  $1S^{2-}$  of Scheme III. However, they are generated after the carboxyl group makes nucleophilic attack at the ester group. Thus,  $1I^0$ ,  $1I^-$ ,  $1I^{-'}$ , and  $1I^{2-}$  of Scheme III contain salicylic acid moieties that readily form metal complexes.<sup>21</sup> Metal complexation of the anhydride intermediates would block the reverse attack of the phenolate ion, leading to a change in the mechanism. Thus, although the spontaneous hydrolysis of  $1S^{2-}$  involves the general-base mechanism ( $k_{12}^{2-}$  step), complexation of metal ions with  $1I^{2-}$  can raise the rate of the nucleophilic path by suppressing the inhibitory reverse attack of the phenolate ion, and the metal ion catalyzed reaction of  $1S^{2-}$  may proceed through the nucleophilic mechanism.

The solvolysis products of **1** obtained in 1:1 (v/v) methanol-

(19) Murakami, Y.; Martell, A. E. *J. Am. Chem. Soc.* **1964**, *86*, 2119.

(20) Stability of  $1I^0$  relative to  $1S^0$  is similar to that of  $1I^{-'}$  relative to  $1S^-$ , and  $k_{12}^0$  is not much different from  $k_{12}^-$ .

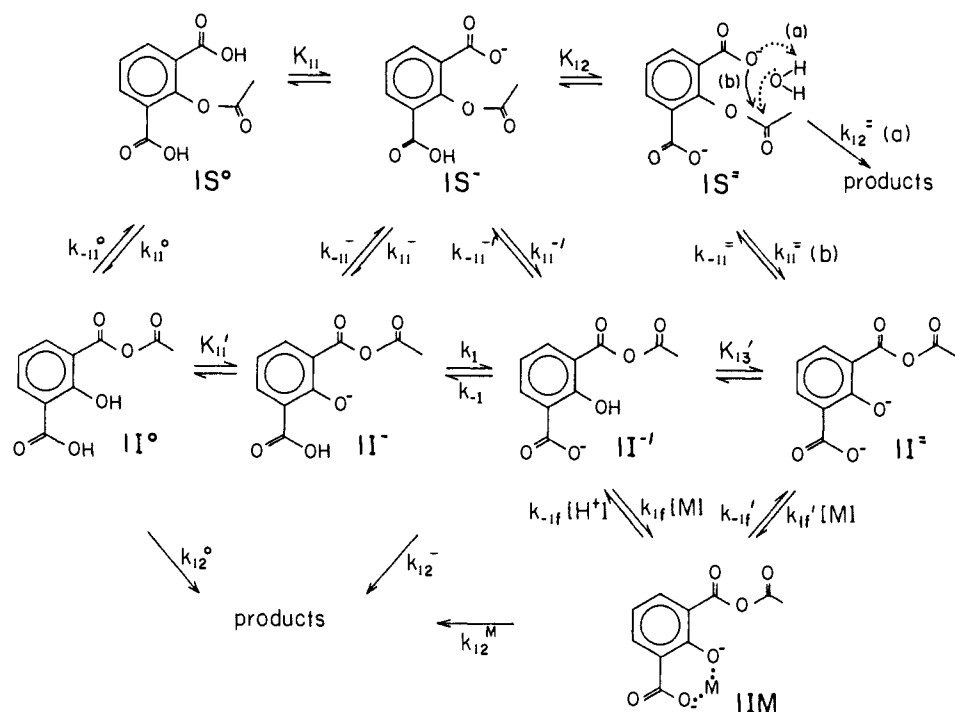
(21) Salicylic acid forms Fe(III) complexes even in acidic solutions, which provides a method of colorimetric identification of salicylic acid: *U.S. Pharmacopeia* **1975**, *19*, p 38.

(16) Fersht, A. R.; Kirby, A. J. *J. Am. Chem. Soc.* **1968**, *90*, 5826.

(17) Fersht, A. R.; Kirby, A. J. *J. Am. Chem. Soc.* **1967**, *89*, 4857.

(18) Kirby, A. J.; Fersht, A. R. *Prog. Bioorg. Chem.* **1971**, *1*, 1.

Scheme III



water in the presence of Fe(III) ion at pH 2.4 (Table III) indicate that an anhydride intermediate is involved in the metal ion catalyzed hydrolysis of **1**. Therefore, the metal ion catalyzed reaction can be represented by the paths involving **IIM** in Scheme III.

The pseudo-first-order rate constant ( $k_0$ ) obtained in the presence of Fe(III) ion is proportional to [Fe(III)] as illustrated in Figure 2, indicating that Fe(III) ion is included in the rate-determining transition state. Therefore, the rate-determining step is either the formation or breakdown of **IIM** under the experimental conditions. Then,  $k_0$  is expressed as eq 1. The first and the second terms of  $\alpha$  (eq 2) represent the reaction paths involving **II'⁻** and **II²⁻**, respectively.

$$k_0 = k_{12}^M[M]\alpha / (k_{12}^M + k_{-1f}[H^+] + k_{-1f}')\beta \quad (1)$$

$$\alpha = k_{1f}k_{11}^{-'} / k_{-11}^{-'} + k_{1f}'k_{11}^{-2}K_{12} / k_{-11}^{-2}[H^+] \quad (2)$$

$$\beta = 1 + [H^+] / K_{11} + K_{12} / [H^+] \quad (3)$$

The pH dependence of the proportionality constant  $k_0/[M]$  obtained for the Fe(III)-catalyzed reaction was analyzed in terms of either eq 4 or 5, both of which are approximated forms derived

$$k_0/[M] = (k_{1f}k_{11}^{-'} / k_{-11}^{-'}) / \beta \quad (4)$$

$$k_0/[M] = (k_{1f}'k_{11}^{-2}K_{12} / k_{-11}^{-2}[H^+]) / \beta \quad (5)$$

from eq 1. It is assumed that  $k_{12}^M \gg k_{-1f}[H^+] + k_{-1f}'$  in both eq 4 and 5.<sup>22</sup> In derivation of eq 5, it is assumed that the reaction proceeds mainly through **II²⁻** (excluding **II'⁻**). Analysis with eq 5 leads to steep curves such as curve B of Figure 3, indicating that **II'⁻** is involved as an intermediate in the metal-catalyzed reactions. In derivation of eq 4, it is assumed that **II'⁻** is the main intermediate. Analysis with eq 4 leads to a good fit ( $k_{1f}k_{11}^{-'} / k_{-11}^{-'} = 0.29 \text{ M}^{-1} \text{ s}^{-1}$ ;  $pK_{11} = 2.85$  and  $pK_{12} = 3.80$  as reported in ref 19) as illustrated in Figure 3.

The good fit of the pH profile of  $k_0/[M]$  to eq 4 indicates that the contribution of the reaction path involving **II²⁻** is not ap-

preciable over the pH range examined. In addition, it reveals that  $k_{12}^M$  can be taken as being much greater than  $k_{-1f}[H^+]$  or  $k_{-1f}'$ , with the rate-determining step being the formation of **IIM**.<sup>22,23</sup> The general expression of  $k_0$  under the condition of  $k_{12}^M \gg k_{-1f}[H^+] + k_{-1f}'$  is derived as eq 6. When  $k_{1f}[M] \ll k_{-11}^{-'}$  and

$$k_0 = k_{11}^{-'}k_{1f}[M] / (k_{-11}^{-'} + k_{1f}[M])\beta + k_{11}^{-2}k_{1f}'K_{12}[M] / (k_{-11}^{-2} + k_{1f}'[M])[H^+]\beta \quad (6)$$

$k_{1f}'[M] \ll k_{-11}^{-2}$  at sufficiently low [M],  $k_0$  is proportional to [M] (eq 7). On the other hand, the nucleophilic attack of the car-

$$k_0/[M] = k_{11}^{-'}k_{1f} / k_{-11}^{-'}\beta + k_{11}^{-2}k_{1f}'K_{12} / k_{-11}^{-2}[H^+]\beta \quad (7)$$

$$k_0 = (k_{11}^{-'} + k_{11}^{-2}K_{12} / [H^+]) / \beta \quad (8)$$

boxylate group at the ester carbon ( $k_{11}^{-'}$  and  $k_{11}^{-2}$  steps) to form the anhydride intermediate becomes rate determining at sufficiently high [M] ( $k_{1f}[M] \gg k_{-11}^{-'}$  and  $k_{1f}'[M] \gg k_{-11}^{-2}$ ). Then,  $k_0$  becomes independent of [M] (8).

Because of the relatively large solubility of the Al(III) ion in water, the Al(III)-catalyzed hydrolysis of **1** was kinetically investigated up to pH 4.2. At pH  $\leq 3.3$ , the rate data were collected up to 0.1 M Al(III). As illustrated in Figure 4,  $k_0$  depends nonlinearly on [Al(III)] and apparently approaches a constant value at high [Al(III)]. This may be related to eq 6, which predicts saturation kinetic behavior with respect to [M]. Then, the limiting value of  $k_0$  at high [M] is given by eq 8. The interpretation of the nonlinear dependence of  $k_0$  on [Al(III)] in terms of eq 6, however, is not consistent with the results obtained with the Fe(III)-catalyzed reaction. For curves B–F of Figure 4, which were obtained for the Al(III)-catalyzed reaction, the limiting values of  $k_0$  appear to be  $(1-3) \times 10^{-4} \text{ s}^{-1}$  at pH  $\leq 3.8$ . On the other hand, deviation of  $k_0$  from the linear dependence on [M] is not evident for the Fe(III)-catalyzed reaction in which observed values of  $k_0$  reach  $(1-3) \times 10^{-4} \text{ s}^{-1}$  at pH  $\leq 3.1$ . Thus, the limiting values of  $k_0$  should be much greater than  $(1-3) \times 10^{-4} \text{ s}^{-1}$  for the Fe(III)-catalyzed reactions in marked contrast with the Al(III)-catalyzed reaction. The limiting value of  $k_0$ , however, should be the same for both Fe(III)- and Al(III)-catalyzed reactions, as indicated by eq 8. The nonlinear dependence of  $k_0$  on [Al(III)]

(22) The formation constants for the 1:1 metal complexes of salicylate dianion ( $\text{Sal}^{2-}$ ) are  $2.5 \times 10^{16}$ ,  $1.3 \times 10^{14}$ , and  $4.3 \times 10^{10} \text{ M}^{-1}$ , respectively, for  $\text{FeSal}^+$ ,  $\text{AlSal}^+$ , and  $\text{CuSal}$ : Yatsimirskii, K. B.; Vasil'ev, V. P. *Instability Constants of Complex Compounds*; Pergamon: London, 1960; p 163. If similar formation constants ( $k_{1f}'/k_{-1f}'$ ) are assumed for **IIM**,  $k_{1f}'$  for the Fe(III) or Al(III) complexes should be smaller than  $10^{-4} \text{ s}^{-1}$  even if the  $k_{1f}$ /step is diffusion controlled. Thus,  $k_{-1f}'$  should be much smaller than  $k_{12}^M$ , which represents the hydrolysis of an anhydride.

(23) If  $k_{-1f}[H^+]$  is comparable to or greater than  $k_{12}^M$ , the pH profile of  $k_0/[M]$  should be much steeper than the observed curve as illustrated in Figure 3 (curve C vs. curve A).

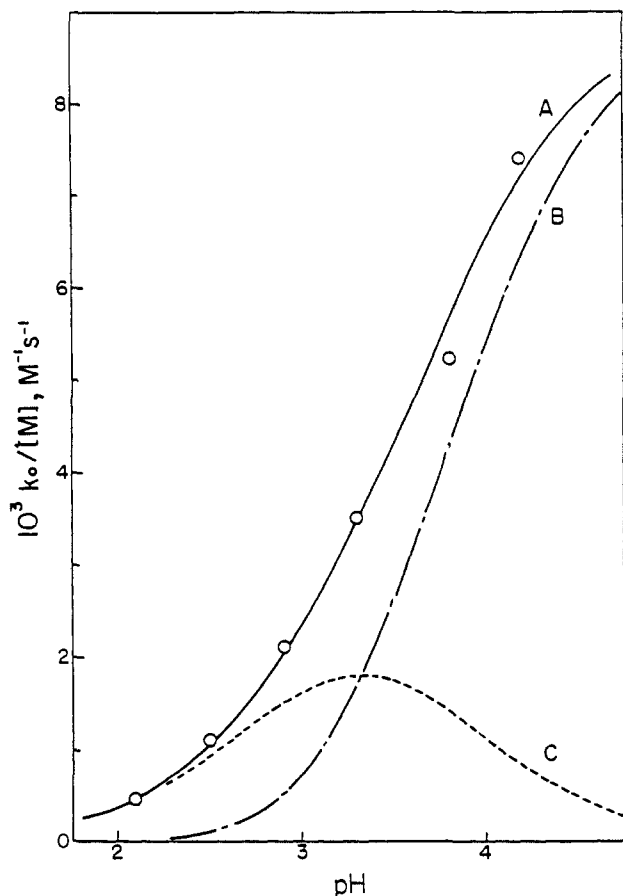


**Figure 6.** pH profile of the slope ( $k_0/[M]$ ) of the straight lines obtained from the data measured at  $[Al(III)] < 0.05$  M (Figure 3). Curve A is constructed according to eq 7 by using  $k_{11}^-k_{1f}/k_{-11}^- = 0.003$   $M^{-1} s^{-1}$  and  $k_{11}^{2-}k_{1f}'/k_{-11}^{2-} = 0.009$   $M^{-1} s^{-1}$  as well as the  $pK_{11}$  (2.85) and  $pK_{12}$  (3.80) values reported in ref 19. Curve B represents the contribution of the reaction path involving  $1S^{2-}$  and curve C that involving  $1S^-$ .

is evident only for the rate data obtained with 0.05–0.01 M Al(III). Since the data were measured at ionic strength 0.6, only small amounts of NaCl were added to the reaction media (no NaCl in 0.1 M AlCl<sub>3</sub> solutions and 0.3 M NaCl in 0.05 M AlCl<sub>3</sub> solutions). Therefore, it is possible that the rate data measured with 0.1–0.05 M Al(III) reflect certain rate-retarding salt effects by AlCl<sub>3</sub>.

When the  $k_0$  values obtained at  $[Al(III)] < 0.05$  M are considered,  $k_0$  is proportional to  $[M]$ . The values for the proportionality constant ( $k_0/[M]$ ) thus obtained are plotted against pH in Figure 6. The theoretical curve of this figure is constructed according to eq 7 by using  $k_{11}^-k_{1f}/k_{-11}^- = 0.003$   $M^{-1} s^{-1}$  and  $k_{11}^{2-}k_{1f}'/k_{-11}^{2-} = 0.009$   $M^{-1} s^{-1}$  as well as the reported values<sup>19</sup> of  $pK_{11}$  (2.85) and  $pK_{12}$  (3.80).<sup>24</sup>

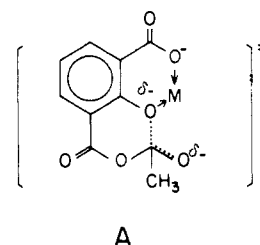
The efficiency of the metal ion catalysis is in the order of Fe(III) > Al(III) >> Cu(II) ~ Zn(II). This order parallels the formation constants for the salicylate complexes of the metal ions.<sup>22</sup> This

(24) According to the analysis made in ref 18,  $k_{21}^0/k_{-21}^0$  (Scheme I) is in the range of  $10^{-6}$  and  $k_{21}^-/k_{-21}^-$  in the range of  $10^{-11}$  for **2a**. If  $k_{11}^-/k_{-11}^-$  (Scheme III) is also taken as ca.  $10^{-6}$ , the values of  $k_{11}^-k_{1f}/k_{-11}^-$  estimated from the pH profiles of Figures 3 and 6 lead to the  $k_{1f}$  values of ca.  $3 \times 10^5$  and  $3 \times 10^3$   $M^{-1} s^{-1}$ , respectively, for the Fe(III)- and Al(III)-catalyzed reactions. If the unfavorable electrostatic interaction between the two adjacent anions in  $1I^{2-}$  is considered,  $k_{11}^{2-}/k_{-11}^{2-}$  (Scheme III) should be smaller than  $k_{21}^-/k_{-21}^-$  (Scheme I) of **2a**. Then,  $k_{1f}'$  for the Al(III)-catalyzed reaction should be greater than  $10^9$   $M^{-1} s^{-1}$  as  $k_{11}^{2-}k_{1f}'/k_{-11}^{2-}$  is  $0.009$   $M^{-1} s^{-1}$ , approaching the diffusion-controlled limit. Even if the diffusion-controlled value of  $k_{1f}'$  is assumed for the Fe(III)-catalyzed reactions,  $k_{11}^{2-}k_{1f}'/k_{-11}^{2-}$  would not be much different for the Fe(III)- and the Al(III)-catalyzed reactions, while  $k_{11}^-k_{1f}/k_{-11}^-$  is about 100 times greater for the Fe(III)-catalyzed reaction. Then, the overall rate ( $k_{11}^{2-}k_{1f}'/k_{-11}^{2-} = 0.01$ – $0.1$   $M^{-1} s^{-1}$  as estimated here) for the Fe(III)-catalyzed hydrolysis of  $1S^{2-}$  would be slower than that ( $k_{11}^-k_{1f}/k_{-11}^- = 0.29$   $M^{-1} s^{-1}$  as estimated from Figure 3) of  $1S^-$ , and this explains why the reaction path involving  $1I^{2-}$  does not contribute appreciably to the pH profile illustrated in Figure 3 at pH  $\leq 3.1$ .

is again consistent with the  $k_{1f}$  and  $k_{1f}'$  steps of Scheme III being the rate-determining step in the metal ion catalyzed hydrolysis of **1** under the experimental conditions.

As discussed in the preceding section, the rate-determining step for the spontaneous hydrolysis of  $3S^-$  (Scheme II) is the nucleophilic attack by the carboxylate group ( $k_{31}^-$  step) to form  $3I^-$ . The value of  $k_{31}^-$  was about  $1.3 \times 10^{-2}$   $s^{-1}$  at 25 °C. As indicated previously, the attack of the carboxylate anion at the acetoxy group in  $1S^-$  or  $1S^{2-}$  appears to be little affected sterically by the presence of the other carboxyl group. Then  $k_{11}^-$ ,  $k_{11}^-'$ , or  $k_{11}^{2-}$  (Scheme III) would not be much different from  $1.3 \times 10^{-2}$   $s^{-1}$ . This value, therefore, represents the maximum value of  $k_0$  (eq 8) that can be attained at sufficiently large  $[M]$  for the metal ion catalyzed hydrolysis of **1**.

The kinetic data measured for the Fe(III)- or Al(III)-catalyzed hydrolysis of **1** may be related to the rate-determining breakdown (A) of the tetrahedral intermediate that leads to the metal-bound



anhydride intermediate (**IIM**) directly from the substrate. This alternative mechanism, however, can be excluded on the following ground. It predicts that the metal ion catalysis would occur mainly with  $1S^{2-}$  in which both of the carboxyl groups are ionized. One carboxylate anion is needed for the nucleophilic attack, and the other is utilized in the metal chelation. Thus, the efficient hydrolysis of  $1S^-$  observed in the presence of Al(III) and especially of Fe(III) is not compatible with the alternative mechanism.

Although  $k_0$  might be raised up to a limiting value of ca.  $1 \times 10^{-2}$   $s^{-1}$  as discussed previously, the kinetic measurements were limited to low metal concentrations due to the limited solubility of the metal ions. Even at low metal concentrations,  $k_0$  values up to  $3 \times 10^{-4}$   $s^{-1}$  are achieved and the degree of acceleration is remarkable. At pH 2.5,  $k_0$  for the spontaneous reaction is  $1.7 \times 10^{-6}$   $s^{-1}$ , while the addition of 4 mM Fe(III) at pH 2.4 increases  $k_0$  to  $2.6 \times 10^{-4}$   $s^{-1}$ . At pH 4.2,  $k_0$  is  $1.5 \times 10^{-4}$   $s^{-1}$  in the presence of 0.02 M Al(III). The major part of this value (88% as estimated in Figure 6) represents the hydrolysis of dianionic species  $1S^{2-}$ . For the spontaneous hydrolysis of  $1S^{2-}$ ,  $k_0$  should be smaller than  $2 \times 10^{-7}$   $s^{-1}$  (Figure 1). Since Al(III)-catalyzed reaction is faster for  $1S^{2-}$  compared with  $1S^-$  while the spontaneous reaction is much slower for  $1S^{2-}$ , the degree of acceleration in the presence of the metal ion is much greater for  $1S^{2-}$ .

In the spontaneous hydrolysis of monoanionic species  $1S^-$ , the inhibitory reverse attack by the phenolate ion in the anhydride intermediate is blocked by the intramolecular proton transfer from the carboxyl group. This leads to the stabilization of the anhydride intermediate, whose breakdown process is the rate-determining step. In the metal ion catalyzed hydrolysis of  $1S^-$ , the anhydride intermediate is further stabilized by metal chelation, which leads to the enhancement in the overall rate.

On the other hand, the inhibitory reverse attack by the phenolate ion is not blocked at all in the spontaneous hydrolysis of dianionic species  $1S^{2-}$ . Consequently, the reaction proceeds through the general-base mechanism. The rate for the nucleophilic path in the spontaneous hydrolysis of  $1S^{2-}$  must be much slower than the observed rate. The degree of rate enhancement achieved by the trivalent metal ions in the nucleophilic path for the hydrolysis of dianionic species  $1S^{2-}$  is, therefore, very large. This catalytic effect originates from the blocking by the metal ions of the inhibitory reverse attack of the phenolate group in  $1I^{2-}$ .

The blocking of the inhibitory reverse paths in the hydrolysis of **1** is achieved by either the intramolecular proton transfer from a carboxyl group or chelation by metal ions. The rate for the spontaneous hydrolysis of monoanionic species  $1S^-$  represents the

efficiency of the blocking by the intramolecular proton transfer, and the rate for the metal-catalyzed hydrolysis of dianionic species  $1S^{2-}$  stands for that by metal chelation. Comparison of these rates indicates that the blocking of the inhibitory reverse path is achieved much more efficiently by complexation with the trivalent metal ions compared with the intramolecular proton transfer.

**Implications to Metalloenzymes.** The majority of enzymatic reactions involve covalent intermediates.<sup>25</sup> When the enzymatic process is a substitution reaction, the leaving group of the substrate remains in the vicinity of the reaction site after it is cleaved by the attack of the enzymatic group. The reverse attack of the leaving group at the resultant intermediate, however, should be also very efficient if the leaving group remains in close proximity to the reaction site. Since this retards the overall reaction, the enzyme must separate the leaving group from the reaction site or block the reactivity of the leaving group.

The aspirin derivatives can be viewed as a model for enzyme–substrate complexes. The carboxyl group of an aspirin derivative corresponds to a catalytic group of an enzyme and the acetoxy moiety to the bound substrate. The phenolate group represents the leaving group of the substrate, which should be blocked or separated after cleavage from the ester linkage in order to achieve fast overall rate. The spontaneous reactions of  $1S^-$  and  $3S^-$  involve intramolecular proton transfer to the phenolate ion from adjacent carboxyl groups. Thus, in the enzymatic processes, proton transfer from an enzymatic group to the leaving group during a substitution process would block the reverse attack by the leaving group. It is noteworthy that carboxyl groups are the most acidic functional groups that are normally available to enzymes.

The metal ion catalysis in the hydrolysis of **1**, especially  $1S^{2-}$  indicates that metal complexation of the leaving group can block the inhibitory reverse paths. Furthermore, the blocking by the metal ions is much more efficient than the intramolecular proton

transfer in the present study. Thus, metal ions of some metalloenzymes might participate in catalysis by blocking the inhibitory reverse paths through binding at the leaving groups. The concentrations of the metal ions are low in the present study; but, the effective concentration of an active-site metal ion is much greater, and the blocking of the inhibitory reverse paths by the active-site metal ion would be much more efficient than that in the present study.

A variety of metalloenzymes have been discovered in which metal ions participate as Lewis acids.<sup>26</sup> Although extensive studies have been performed on some of the metalloenzymes<sup>1</sup> such as carboxypeptidase A and carbonic anhydrase, the exact roles of the active-site metal ions are unknown.<sup>9,27,28</sup> For many metalloenzymes, various roles have been assigned to the metal ions,<sup>25–28</sup> but the assignment is based mostly on speculation. This is because no decisive physical method is currently available for correct assignment of the catalytic roles of the active-site metal ions. In this regard, the catalytic features disclosed by the studies with small molecules are particularly useful in the study of metalloenzymes. Catalysis by blocking inhibitory reverse paths is a novel catalytic factor for metal ions. This can be utilized not only in the study of inorganic or organic reaction mechanisms but also in the discussion of the mechanistic roles of metal ions in various metalloenzymes.

**Acknowledgment.** This work was supported by a grant from the Korea Science and Engineering Foundation.

**Registry No.** 1, 90772-05-7;  $FeCl_3$ , 7705-08-0;  $CuCl_2$ , 7447-39-4;  $ZnCl_2$ , 7646-85-7; 3-carboxysalicylic acid, 606-19-9; dimethyl 3-carboxysalicylate, 36669-06-4; methyl 3-carboxysalicylate, 101670-85-3; aluminum chloride, 7446-70-0.

(26) Galdes, A.; Hill, H. A. O. *Inorganic Biochemistry*; Hill, H. A. O., Ed.; The Chemical Society: London, 1979; Vol. 1, Chapter 8.

(27) Golding, B. T.; Leigh, G. J. *Inorganic Biochemistry*; Hill, H. A. O., Ed.; The Chemical Society: London, 1979; Vol. 1, Chapter 2.

(28) Pocker, Y.; Sarkanian, S. *Adv. Enzymol.* **1978**, *47*, 149.

(25) Spector, L. B. *Covalent Catalysis by Enzymes*; Springer-Verlag: New York, 1982.

## Structure of Aridicin A. An Integrated Approach Employing 2D NMR, Energy Minimization, and Distance Constraints

Peter W. Jeffs,\* Luciano Mueller, Charles DeBrosse, Sarah L. Heald, and Richard Fisher

Contribution from Smith Kline and French Laboratories, Philadelphia, Pennsylvania 19101.  
Received July 5, 1985

**Abstract:** Elucidation of the structures of aridicin aglycon (**2**) and the parent antibiotic, aridicin A (**8**), are described. Two-dimensional NMR correlation spectroscopy (COSY) and nuclear Overhauser spectroscopy (NOESY) in conjunction with an improved delayed COSY sequence are utilized together with previous chemical data to elucidate the covalent structural framework of the aglycon. Elaboration of the latter to a full three-dimensional structure representing a minimum energy conformation **6** is described by using intramolecular hydrogen–hydrogen distance information derived from the 2D NOE results in conjunction with interactive computer-assisted molecular modeling and force field energy minimization. The full details of positions and stereochemistries of the attachment of mannose and the 2-deoxy-2-[(1-oxodecyl)amino]-D-glucopyranosiduronic acid residue in aridicin A by two-dimensional NMR methods including double quantum experiments are described.

Glycopeptide antibiotics belonging to the vancomycin–ristocetin class<sup>1</sup> have been the subject of much recent interest, owing to the increasing importance of vancomycin for the treatment of methicillin-resistant staphylococcal infections<sup>2</sup> and pseudomem-

branous colitis<sup>3</sup> plus the development of certain members of these glycopeptides as growth-promotant feed additives for livestock.<sup>4</sup>

The glycopeptide antibiotics exert their biological action by inhibiting bacterial cell wall synthesis by binding to putative cell wall precursors that terminate in L-Lys-D-Ala-D-Ala. The an-

(1) Williams, D. H.; Rajanada, V.; Williamson, M. P.; Bojesen, G. In *Topics in Antibiotic Chemistry*, Part B; Sammes, P., Ed.; Ellis Horwood: Chichester, U.K., 1980; Vol. 5, pp 119–158.

(2) Karchmer, A. W.; Archer, G. L.; Dismukes, W. *Ann. Int. Med.* **1983**, *98*, 477–485.

(3) Cafferkey, M. T.; Hine, R.; Keane, C. T. *J. Antimicrob. Chemother.* **1982**, *9*, 69–74.

(4) Fesik, S. W.; Armitage, I. M.; Ellstad, G. A.; McGahren, W. J. *Mol. Pharmacol.* **1984**, *25*, 275–280.